Journal of Materials Chemistry

Cite this: J. Mater. Chem., 2012, 22, 4306

www.rsc.org/materials

PAPER

Supramolecular polymeric nanowires: preparation and orthogonal modification of their photophysical properties†

Ting Lei,[a] Chu-Yang Cheng,[a] Zi-Hao Guo,[a] Cui Zheng,[b] Ye Zhou,[a] Dehai Liang*[b] and Jian Pei*[a]

Received 24th August 2011, Accepted 4th October 2011
DOI: 10.1039/c1jm14138d

A series of three-dimensional shape-persistent molecules with three conjugated arms perpendicular to a planar core were developed to self-assemble into supramolecular polymeric nanowires through multiple hydrogen-bonding interactions. After introducing bulky functional groups, aggregation of the nanowires was inhibited, and single molecular nanowires were obtained in concentrated solutions. Therefore, these nanowires had large surface areas with functional groups appended on the surface. Moreover, the photophysical properties of the functional groups including emission peaks and fluorescent lifetime were not changed after self-assembly. Some nanowires emitted high fluorescence after incorporating various chromophores on the side chains of the three-dimensional skeleton through effective fluorescence resonance energy transfer. For example, **1-BTHex** showed a quantum efficiency of about 7.9% in solution, similar to the model compound **DHBT**. However, in the solid state the fluorescence of **DHBT** was almost quenched with a quantum efficiency lower than 1% due to π–π interactions, but **1-BTHex** also gave much higher quantum efficiency, about 6%, which was close to that in solution.

Introduction

Organic nanowires (ONWs) have attracted increasing attention because they open up a new bottom-up approach to fabricate nano-optoelectronic devices,[1] including explosive detectors,[2] organic field effect transistors,[3] and others.[4] Recently, π–π interactions have provided an excellent approach to form organic nanowires in many systems through various growing conditions.[1–4] Owing to the complexity, weakness, and low directionality of π–π interactions,[5–9] the growing conditions of nano/microstructures always change after introducing functional groups, and the expected morphologies are sometimes difficult to realize. Therefore, controlled growth and preparation of nanowires or even single molecular wires with special functional groups to realize certain properties are still of great challenges.

In our previous work, we developed a novel supramolecular polymer constructed by multiple hydrogen-bonding interactions, which formed uniform nanowires with high solid quantum efficiency.[10] As shown in Fig. 1, our three-dimensional skeleton has a shape-persistent structure with three conjugated arms perpendicular to a planar core, in which both R_1 and R_2 are modified with functional groups and the direction of three arms is the self-assembly direction. Herein, we present the synthesis of a series of side chain functionalized monomers, which also form supramolecular polymers through hydrogen bonding. Four different functional moieties are introduced to modify the photophysical properties of the desired nanowires. The fluorescence resonance energy transfer (FRET) principle was applied to choose chromophores on the side chains. We chose benzothiadiazole and porphyrin units as the emitting groups, because their absorption features match well with the emission of the skeleton. The introduction of the functional groups on the side chains does not change their one-dimensional growth tendency, and the

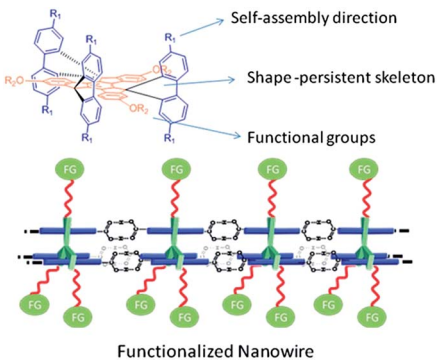

Fig. 1 The design strategy of the functional supramolecular polymers.

[a]Beijing National Laboratory for Molecular Sciences (BNLMS) Key Labs of Bioorganic Chemistry College of Chemistry and Molecular Engineering, Peking University, Beijing, 100871, China. E-mail: jianpei@pku.edu.cn; Fax: (+86) 10-62751845; Tel: (+86) 10-62751845
[b]Key Laboratory of Polymer Chemistry and Physics of the Ministry of Education, College of Chemistry and Molecular Engineering, Peking University, Beijing, 100871, China

† Electronic Supplementary Information (ESI) available: Data of the experiment details, ^{1}H NMR spectra, ^{13}C NMR spectra and MALDI-TOF. See DOI: 10.1039/c1jm14138d

monomers can easily self-assemble into supramolecular polymeric nanowires. Interestingly, single molecular wires are also obtained from concentrated solutions due to steric hindrance of the chromophores. Moreover, the nanowires emit different colors depending on the attached chromophores. The introduction of various chromophores can also test our assumption about whether this strategy might have broad applications for different types of functional groups.

Results and discussion

Synthesis

Scheme 1 illustrates the synthesis routes for the functionalized monomers. Compound **2** was readily obtained through four steps from commercially available materials, as described in our previous report.[11] A demethylation reaction of **2** using BBr_3 was smoothly performed at room temperature and then followed by an alkylation with 12-bromododecan-1-ol to afford **3** in 79% yield. Firstly, PBr_3 was employed to convert hydroxyl groups to bromide terminal groups, which resulted in very low yield. Then we used 4-toluenesulfonyl chloride to convert hydroxyl groups to achieve tosylate ester **4**. A Suzuki–Miyaura coupling reaction was carried out between **4** and 4-methoxycarbonylphenylboronic pinacol ester to afford **5**. The usage of the more active palladium catalyst $Pd_2(dba)_3$ and the ligand PCy_3 led to 73% yield. Compound **5** reacted with **TPPOH**, **TPABTOH**, **HexBTOH**, and **MeBTOH** using K_2CO_3 in DMF following a hydrolysis reaction using LiOH to afford the target monomers, **1-TPP**, **1-BTTPA**, **1-BTHex**, and **1-BTMe**, in high yields. All the compounds are readily soluble in THF, and show low solubility in CH_2Cl_2, $CHCl_3$, and hexane. Furthermore, we also synthesized a model compound **DHBT** to understand the photophysical properties (Scheme 2).

Nanowire growth and characterization

We used a vapor-diffusion strategy to grow nanowires. These compounds were firstly dissolved in THF to form homogenous solutions, and then CH_2Cl_2 was introduced by gradual vapor

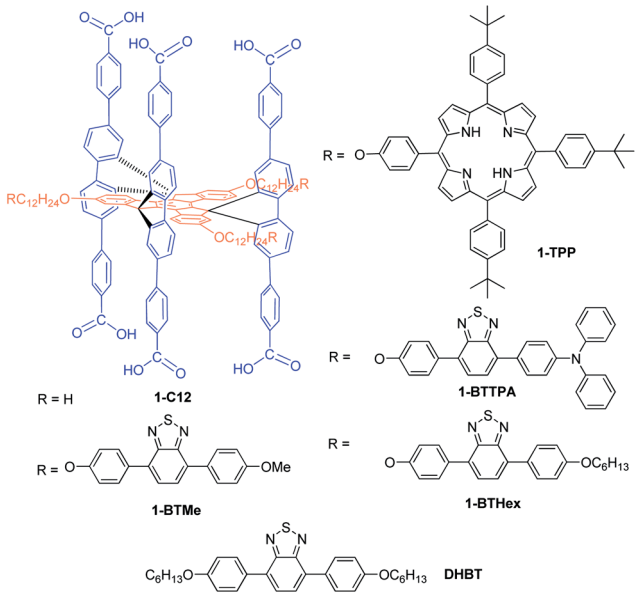

Scheme 2 Structures of the self-assembling monomers used in this study.

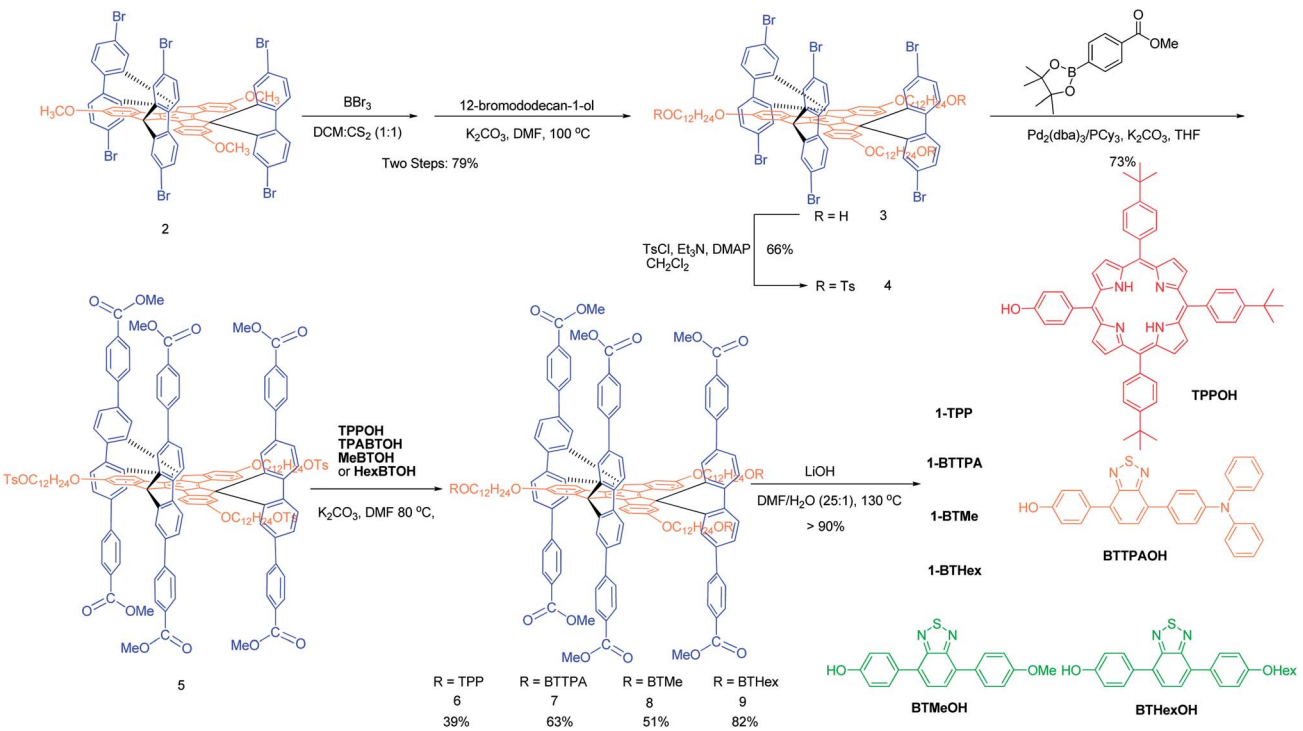

Scheme 1 Synthesis routes for the functionalized monomers.

diffusion to decrease the solubility of the compound. Scanning electron microscopy (SEM) was employed to investigate the formed aggregates (Fig. 2). SEM images show that all the monomers formed well-defined nanowires which are hundreds of nanometres wide and micrometres long. This result is rarely reported in previous literature,[1–4] because even for a small change in the molecular structure, the self-assembly morphology dramatically changes.[1a,b] In our system, the 1D growth tendency was retained well because the hydrogen-bonding interaction was strong and the bonding sites were isolated from the "external environment" by the shape-persistent skeleton.

Transmission electron microscopy (TEM) and atomic force microscopy (AFM) were also employed to investigate the formation of the nanowires. As shown in Fig. 3, nano/microwires of **1-TPP** and **1-BTTPA** were formed with bundles of smaller nanowires of several nanometres in width. Similar results were also observed in AFM images (Fig. 4), at larger scale, **1-TPP** and **1-BTTPA** formed wires ranging from tens to hundreds of nanometres in width. A detailed analysis by AFM reveals that nanowires of **1-TPP** had a smallest height of 3.5 nm and those of **1-BTTPA** showed a smallest height of 3.8 nm (white arrows in Fig. 4b and d), which agreed well with the molecular size given by molecular modeling (Fig. 5). This is direct evidence of the existence of single molecular wires. We also observed the side attached single molecular wires as shown by the red arrows. These result demonstrated that these nano/microwires were formed through the side-by-side attachment of single molecular wires. Previously, we reported the formation of single molecular wires in highly diluted solution (10^{-6} M),[10] and we assumed that the nanowires were formed by the packing of lots of single molecular wires. However, herein the single molecular wires were found in highly concentrated solutions (10^{-4} M), and their packing was also observed from AFM images, which proved our previous assumption. Unlike flexible dodecyl chains in **1-C12**, we considered that the bulky functional groups of the molecules hindered the fusion of single molecular wires into larger assemblies. Therefore, we obtained the single molecular wires in concentrated solutions.

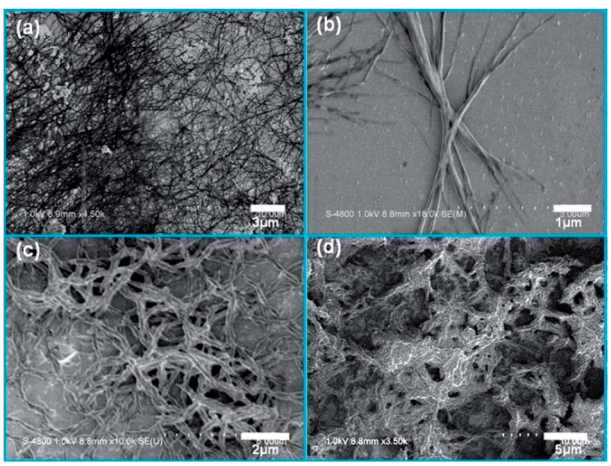

Fig. 2 SEM images of the morphologies formed by (a) **1-TPP**; (b) **1-BTTPA**; (c) **1-BTMe**; (d) **1-BTHex** in THF/CH_2Cl_2 at 0.5 mg mL^{-1}.

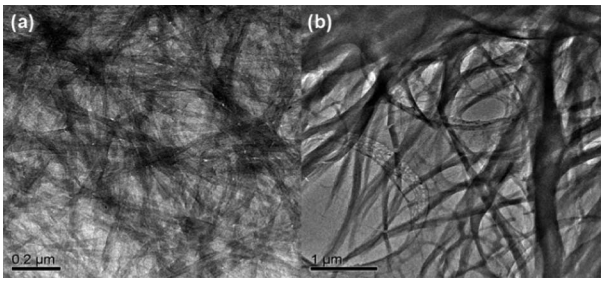

Fig. 3 TEM images of (a) **1-TPP** and (b) **1-BTTPA** nanowires directly drop-cast onto a micro-grid.

Photophysical properties and FRET process

The photophysical features of the monomers and nanowires were investigated in detail and are summarized in Table 1. As illustrated in Fig. 6, the absorption spectra of the monomers in solution exhibited two main absorption peaks, one from the main skeleton (around 322 nm) and another from the functionalized side groups (around 400–450 nm). When excited at the maximum absorption of the skeleton (around 322 nm) of the monomers, the emission from the functionalized side groups appeared, and the emission from the skeleton was dramatically quenched. These results indicated that intramolecular energy transfer processes from the skeleton to the monomers in solution clearly happened. The absorption and emission spectra of the nanowires were also measured by drop-casting their suspensions onto quartz plates. A shoulder in the absorption band of the 3D skeleton was observed, which was attributed to the relatively more rigid skeleton after hydrogen bonding.[10] Noticeably, the absorption peaks of all the side groups remained almost unchanged, indicating the van der Waals interactions, especially π–π interactions, of the side

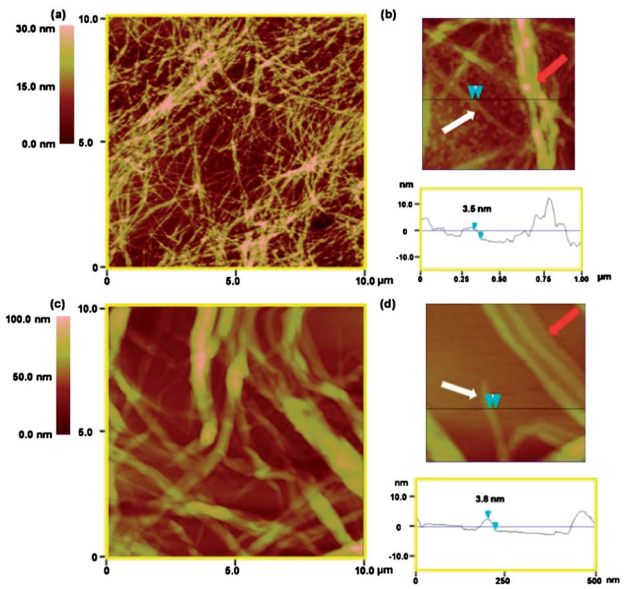

Fig. 4 AFM height images (a, c) at large scale; (b, d) small scale and small scale section analysis of (a, b) **1-TPP**; (c, d) **1-BTTPA** nanowires on mica substrates.

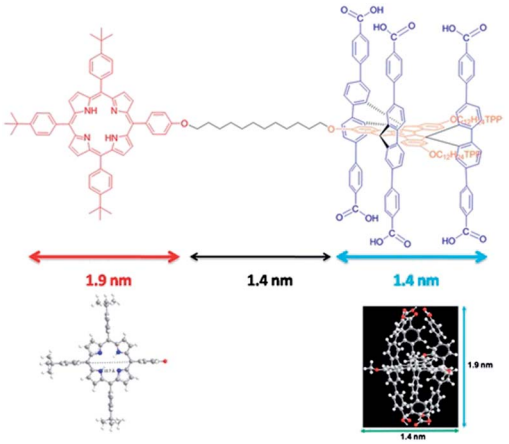

Fig. 5 Estimation of the size of **1-TPP** by molecular modelling (molecular models were minimized using MMFF94 force field).

groups were very weak. Interestingly, because of the narrow absorption of the Soret band (420 nm)[12] of the porphyrin groups, only one vibrational emission was transferred in the process, and the emission from the skeleton was split into two peaks (Fig. 6a).

We also measured the time-resolved fluorescence decays of **1-C12**, **1-BTTPA**, and **1-BTMe** in dilute solution, as summarized in Table 2. When excited at 339 nm, **1-C12** showed a fluorescent lifetime of 1.24 ns (69%) and 8.2 ns (31%). In contrast, the fluorescent lifetime of the skeleton (monitored at 411 nm) dramatically decreased in **1-BTTPA** and **1-BTMe** (Fig. 7). The measured fluorescent lifetimes were 1.0 ns (81%), 2.1 ns (19%) for **1-BTTPA** and 1.1 ns (92%), 2.7 ns (8%) for **1-BTMe**. The dramatic decrease of the lifetime of the main skeleton suggested that the energy transfer was not a trivial energy transfer (radiative energy transfer). Meanwhile, because the skeleton and the functional groups are well separated with non-conjugated aliphatic chains, the energy transfer did not follow the Dexter mechanism but rather the Förster mechanism. On the other hand, when excited at the absorption of the functional groups of **1-BTMe** (390 nm) and monitored at the emission of the functional groups (526 nm), the fluorescent lifetime was 8 ns, similar to the lifetime of the reference compound **DHBT** (10 ns). Accordingly, the photophysical properties of functional groups, including emission peaks and fluorescent lifetime, are not changed.

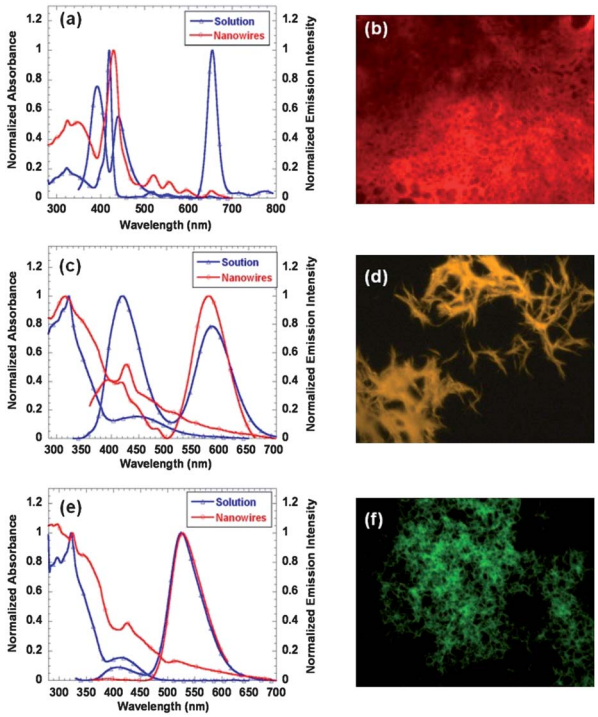

Fig. 6 (a) UV-vis, PL spectra and fluorescence microscopy images of (a, b) **1-TPP**, (c, d) **1-BTTPA**, (e, f) **1-BTMe** in THF solution (1.0×10^{-6} M) or as nanowires. All the monomer emission spectra were excited at the maximum absorption peak of the main skeleton. The emission of **1-TPP** from the solid state was very weak and is not shown in the spectra.

To quantify the energy transfer (ET) efficiency, we measured the fluorescence quantum yields of the donor in the presence and absence of acceptor using eqn (1),[13]

$$\Psi_{ET} = 1 - \frac{Q_{\text{donor (acceptor)}}}{Q_{\text{donor}}} \quad (1)$$

in which Q_{donor} and Q_{acceptor} correspond to the fluorescence quantum efficiency of the donor in the absence and the presence of the acceptor, respectively. Herein, the Q_{donor}, the quantum efficiency of **1-C12**, was 24%. Clearly, **1-BTMe** and **1-BTHex** showed the highest ET efficiencies up to 70% (Table 3), which may be attributed to the perfect match between their absorption and the emission of the main skeleton. The FRET process became much more efficient in the solid state. For **1-BTTPA**, the

Table 1 Summary of the optical properties of the monomers in dilute solution and in nanowires

	In solution (10^{-6} in THF)		Nanowires	
Compound	λ_{abs} (nm)[b]	λ_{emi} (nm)	λ_{abs} (nm)	λ_{emi} (nm)
1-TPP	323 (5.54), 420 (6.22)	392, 440, 655	324, 429	N/A[c]
1-BTTPA	322 (5.07), 449 (4.43)	421, 583	317, 426	577
1-BTMe	322 (5.31), 416(4.54)	408, 526	324, 426	528
1-BTHex	322 (5.47), 420 (4.77)	410, 526	325, 356, 425	529
1-C12[a]	324 (5.18)	411	327	424
DHBT	414 (4.10)	529	420, 520	519

[a] Data come from our previous report. [b] Extinction coefficients, log ε (L^{-1} mol^{-1} cm^{-1}), are shown in parentheses. [c] Not measured, because the peak was very weak.

Table 2 Excitation wavelength (λ_{ex}), monitoring wavelength (λ_{em}) and fluorescence lifetime (τ) obtained from the time-resolved fluorescence measurement in THF solution (10^{-6} M)

Compound	λ_{ex} [nm]	λ_{em} [nm][a]	τ[a]
1-C12	339	411	1.24 ns (69%), 8.2 ns (31%)
1-BTTPA	339	411	1.0 ns (81%), 2.1 ns (19%)
1-BTMe	339	411	1.1 ns (92%), 2.7 ns (8%)
	390	526	8 ns
DHBT	390	526	10 ns

[a] Percentages of different decay lifetimes were calculated and are shown in parentheses.

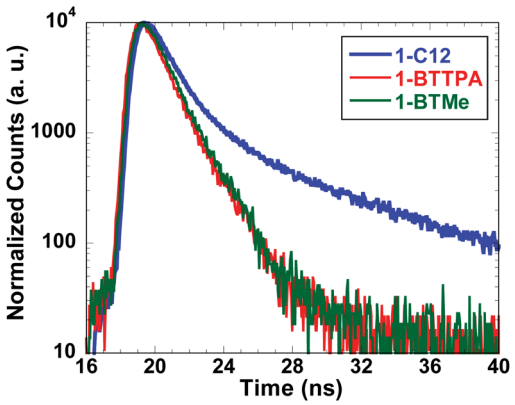

Fig. 7 Time-resolved fluorescence decays of **1-C12**, **1-BTTPA** and **1-BTMe** excited at 339 nm (absorption of the main skeleton), and monitored at 411 nm (emission of the main skeleton). The fluorescence lifetime of the main skeleton were largely shortened because of FRET process.

Table 3 Energy transfer efficiencies measured in solution and in the solid state

Compound	Φ_{FL}[a]	Ψ_{ET}[a]	Φ_{FL}[b]	Ψ_{ET}[b]
1-TPP	9.7%	60%	very low	> 99%
1-BTTPA	18%	25%	7.1%	70%
1-BTMe	7.9%	67%	very low	> 99%
1-BTHex	7.3%	70%	very low	> 99%
1-C12 (donor)	24%	N/A	22%	N/A

[a] Measured at the peak of 410 nm, and using 9,10-diphenylanthracene as the reference in dilute solution. [b] Measured at the solid state using a integrating sphere system. Φ_{FL} is the quenched quantum efficiency of the donor; Ψ_{ET} is the energy transfer efficiency from the skeleton to the side chain chromophores.

energy transfer efficiency increased from 25 to 70%, and for **1-BTMe** and **1-BTHex**, the efficiencies increased from 70 to 99%. These results are attributed to the efficient intermolecular energy transfer in the solid state. Interestingly, the emission from the skeleton showed some fine vibrational structures, indicating that three conjugated arms were solidified by the hydrogen-bonding in self-assembly state (Fig. 6c). Similar to the absorption spectra, the emission from the nanowires exhibited no obvious changes compared with those in the solution. In this system, the properties of the functional groups are well retained, we call it "orthogonal modification". In typical π–π interacting systems, molecules are required to be closely packed (0.34 nm). The strong interactions of the functional groups always change their photophysical or electronic properties. Furthermore, we also measured the quantum efficiency in the solid state. Except **1-TPP**, all the nanowires exhibited much higher quantum efficiencies than their side-chain functional groups. For example, **1-BTHex** showed a quantum efficiency of about 7.9% in solution, similar to model compound **DHBT** in dilute solution. However, in the solid state the fluorescence of **DHBT** was almost quenched with a quantum efficiency lower than 1%, but **1-BTHex** also gave a much higher quantum efficiency of about 6%. This result was both the contribution from the reduced side-chain interactions and the energy transfer from the skeleton.

Conclusions

In summary, we have developed four functionalized monomers which readily self-assemble into supramolecular polymeric nanowires in solution. The three-dimensional monomers have a shape-persistent structure with three conjugated arms perpendicular to a planar core. The conjugated arms are designed to form multiple hydrogen bonds, and the planar core is functionalized to modify their photophysical properties. After the functionalization, all the monomers kept their one dimensional self-assembly tendency very well and formed nano/microwires in solution. Noticeably, single molecular wires were also obtained in a concentrated solution due to the strong hydrogen-bonding interactions and weak intermolecular interactions of the functional groups.

The investigation of their photophysical properties shows that the photophysical properties of the side groups were not affected by the self-assembly in the solid state, which is rarely achieved in π–π interacting systems. The monomers showed clear intramolecular FRET processes both in dilute solution and in the solid state, and the energy transfer efficiencies were also calculated. After they self-assemble into supramolecular nanowires, the intermolecular energy transfers become dominant in the supramolecular nanowires. Except for **1-TPP**, all the nanowires exhibited much higher quantum efficiencies than their side-chain functional groups. For example, the fluorescence of **DHBT** was almost quenched in the solid state with a quantum efficiency lower than 1% due to π–π interactions, but **1-BTHex** gave a much higher quantum efficiency of about 6%, which is close to the value in solution. These organic nanowires have very large surface areas with functional groups appended on the surface. Therefore, they may show potential applications in explosives detection, hazardous gas sensing, and biological applications.

Experimental section

General methods

Chemicals were purchased and used as received. All air and water sensitive reactions were performed under nitrogen atmosphere. Toluene and tetrahydrofuran (THF) were distilled from sodium and benzophenone ketyl. ^{1}H and ^{13}C NMR spectra were recorded on a Varian Mercury plus 300 MHz and Bruker ARX-400 (400MHz). All chemical shifts were reported in parts per million (ppm), ^{1}H NMR chemical shifts were referenced to TMS (0 ppm)

or $CHCl_3$ (7.26 ppm), and ^{13}C NMR chemical shifts were referenced to $CDCl_3$ (77.00 ppm). Absorption spectra were recorded on a PerkinElmer Lambda 35 UV-vis Spectrometer. PL spectra were recorded on a PerkinElmer LS55 Luminescence Spectrometer. MALDI-TOF mass spectra were recorded on a Bruker BIFLEX III time-of-flight (TOF) mass spectrometer (Bruker Daltonics, Billerica, MA, USA) using a 337 nm nitrogen laser with dithranol as the matrix.

Scanning electron microscopy (SEM) images were obtained using a cold field emission scanning electron microscope (FESEM, Hitachi S-4800) operated at an accelerating voltage of 1.0 kV. All the samples were prepared by directly drop-casting the nanowire suspensions on a silicon wafer. Molecular modeling was performed using ChemBio3D Ultra (version 11.0) software available from CambridgeSoft. Energy was minimized using the Merck Molecular Force Field 94 (MMFF94) (convergence criterona: atomic root mean square force 0.001 kcal mol^{-1}). Transmission electron microscopy (TEM) images were obtained using a transmission electron microscope (FEI Tecnai G^2 S-TWIN20) operated at an accelerating voltage of 80 kV and selected area electron diffraction patterns were taken at an accelerating voltage of 200 kV. All the samples were prepared by directly drop-casting the nanowire suspensions on a grid covered with a thin carbon support film. Atomic force microscopy (AFM) studies were performed with a Nanoscope IIIa microscope (Extended Multimode, Digital Instruments, Santa Barbara, CA). All experiments were carried out in tapping mode at ambient temperature. A silicon nitride cantilever was used with a resonance frequency of 306 kHz. The samples were prepared by directly spin-casting the nanowire suspensions on a mica substrate. Fluorescence optical microscopy was performed using an Olympus BX-51 fluorescence optical microscope. Time-resolved fluorescence spectra were measured on a HORIBA Jobin Yvon Fluoromax-4 spectrometer. Solid-state quantum efficiencies were measured on a HORIBA Jobin Yvon Nanolog system.

Acknowledgements

This work was supported by the Major State Basic Research Development Program (Nos. 2006CB921602 and 2009CB623601) from the Ministry of Science and Technology, and National Natural Science Foundation of China.

Notes and references

1 (*a*) Y. S. Zhao, H. Fu, A. Peng, Y. Ma, Q. Liao and J. Yao, *Acc. Chem. Res.*, 2010, **43**, 409; (*b*) L. Zang, Y. Che and J. S. Moore, *Acc. Chem. Res.*, 2008, **41**, 1596; (*c*) J. G. Rudick and V. Percec, *Acc. Chem. Res.*, 2008, **41**, 1641; (*d*) J. Wu, W. Pisula and K. Müllen, *Chem. Rev.*, 2007, **107**, 718; (*e*) A. P. H. J. Schenning and E. W. Meijer, *Chem. Commun.*, 2005, 3245; (*f*) D. T. Bong, T. D. Clark, J. R. Granja and M. R. Ghadiri, *Angew. Chem., Int. Ed.*, 2001, **40**, 988.
2 (*a*) Y. Che, X. Yang, S. Loser and L. Zang, *Nano Lett.*, 2008, **8**, 2219; (*b*) Y. Che, A. X. Y. Datar, T. Naddo, J. Zhao and L. Zang, *J. Am. Chem. Soc.*, 2007, **129**, 6354.
3 (*a*) Q. Tang, Y. Tong, W. Hu, Q. Wan and T. Bjørnholm, *Adv. Mater.*, 2009, **21**, 4234; (*b*) Y. Zhou, W.-J. Liu, Y. Ma, H. Wang, L. Qi, Y. Cao, J. Wang and J. Pei, *J. Am. Chem. Soc.*, 2007, **129**, 12386; (*c*) D. H. Kim, D. Y. Lee, H. S. Lee, W. H. Lee, Y. H. Kim, J. I. Han and K. Cho, *Adv. Mater.*, 2007, **19**, 678; (*d*) Q. Tang, H. Li, Y. Liu and W. Hu, *J. Am. Chem. Soc.*, 2006, **128**, 14634.
4 (*a*) Y. Che, X. Yang, K. Balakrishnan, J. Zuo and L. Zang, *Chem. Mater.*, 2009, **21**, 2930; (*b*) Y. Zhou, L. Wang, J. Wang, J. Pei and Y. Cao, *Adv. Mater.*, 2008, **20**, 3745; (*c*) Y. S. Zhao, H. Fu, A. Peng, W. Yang and J. Yao, *Adv. Mater.*, 2008, **20**, 2859; (*d*) Y. Yamamoto, T. Fukushima, Y. Suna, N. Ishii, A. Saeki, S. Seki, S. Tagawa, M. Taniguchi, T. Kawai and T. Aida, *Science*, 2006, **314**, 1761.
5 (*a*) T. F. A. de Greef, M. M. J. Smulders, M. Wolffs, A. P. H. J. Schenning, R. P. Sijbesma and E. W. Meijer, *Chem. Rev.*, 2009, **109**, 5687; (*b*) F. J. M. Hoeben, P. Jonkheijm, E. W. Meijer and A. P. H. J. Schenning, *Chem. Rev.*, 2005, **105**, 1491.
6 (*a*) R. P. Sijbesma, F. H. Beijer, L. Brunsveld, B. J. B. Folmer, J. H. K. K. Hirschberg, R. F. M. Lange, J. K. L. Lowe and E. W. Meijer, *Science*, 1997, **278**, 1601; (*b*) P. Cordier, F. Tournilhac, C. Soulié-Ziakovic and L. Leibler, *Nature*, 2008, **451**, 977.
7 R. Abbel, C. Grenier, M. J. Pouderoijen, J. W. Stouwdam, P. E. L. G. Leclère, R. P. Sijbesma, E. W. Meijer and A. P. H. J. Schenning, *J. Am. Chem. Soc.*, 2009, **131**, 833.
8 R. M. Capito, H. S. Azevedo, Y. S. Velichko, A. Mata and S. I. Stupp, *Science*, 2008, **319**, 1812.
9 G. Zhang, W. Jin, T. Fukushima, A. Kosaka, N. Ishii and T. Aida, *J. Am. Chem. Soc.*, 2007, **129**, 719.
10 J. Luo, T. Lei, L. Wang, Y. Ma, Y. Cao, J. Wang and J. Pei, *J. Am. Chem. Soc.*, 2009, **131**, 2076.
11 (*a*) J. Luo, Y. Zhou, Z.-Q. Niu, Q.-F. Zhou, Y. Ma and J. Pei, *J. Am. Chem. Soc.*, 2007, **129**, 11314; (*b*) J. Luo, T. Lei, X. Xu, F.-M. Li, Y. Ma, K. Wu and J. Pei, *Chem.–Eur. J.*, 2008, **14**, 3860.
12 H. L. Anderson, *Chem. Commun.*, 1999, 2323.
13 Joseph R. Lakowicz, in *Principles of Fluorescence Spectroscopy* (2nd edition), Plenum Publishing Corporation, 1999.